Polymer Chemistry

ROYAL SOCIETY OF CHEMISTRY

PAPER

View Article Online
View Journal | View Issue

Cite this: *Polym. Chem.*, 2024, **15**, 2959

Vat photopolymerization using catalytic chain transfer polymerization (CCTP) derived reactive oligomers to influence mechanical properties†

Wai Hin Lee, [a,b] Zhongyuan Wan,[b] Ataulla Shegiwal[a] and David Haddleton [*b]

Received 30th April 2024,
Accepted 27th June 2024

DOI: 10.1039/d4py00482e

rsc.li/polymers

ω-Vinyl terminated reactive oligomers of 2-ethylhexyl methacrylate and poly(ethylene glycol)methacrylate (PEGMA) were synthesized *via* catalytic chain transfer polymerization (CCTP) and subsequent addition–fragmentation chain transfer (AFCT) polymerization. The reactive oligomers were then incorporated into 3D-printing resins composed of isobornyl acrylate and poly(ethylene glycol)diacrylate (PEGDA). The formulations were used in digital light processing (DLP) 3D printing, and the mechanical properties of the printed parts evaluated. The effects of concentration, molecular weight and chemistry of the reactive oligomers additives were investigated. It was found that EHMA based reactive oligomers acted as plasticizers resulting in the weakening of the printed objects, whereas PEGMA based reactive oligomers transformed the objects from stiff and brittle to ductile elastomer-like materials.

Introduction

Vat photopolymerization based 3D printing is an emerging technique to fabricate polymeric materials with high resolution and volume within a relatively short time. Compared to other techniques, vat photopolymerization has the advantages of low instrument cost and high robustness towards different materials.[1–3] To tailor the properties and/or functionalize the products, a small quantity of additive can be added to the resin instead of changing the entire formulation. Ideally, a reactive additive is advantageous to avoid leaching and deterioration of properties over time.

Prepolymers are a class of additives commonly employed in curing resins. In essence, polymer is dissolved in the resin as solvent which will incorporate into the objects after curing. However, this method typically required relatively high additive content (up to 50% w/w). Also, increased viscosity and polymerization-induced phase separation can be issues when a high concentration, or high molecular weight of prepolymer is applied.[4–8] One solution is to use reactive low molecular weight reactive prepolymers/oligomers to maintain a low viscosity and miscibility while leaching is mitigated as a result of copolymerization, in contrast to conventional non-reactive small molecular additives.[9,10]

Catalytic chain transfer polymerization (CCTP) is a well-established polymerization technique to synthesise oligomers with a ω-vinyl group using certain low spin Co(II) complexes as chain transfer agents.[11–13] The ω-vinyl terminated oligomers, termed as reactive oligomers, can further copolymerize with other monomers to obtain graft/block architectures and therefore are good candidates for reactive (polymerizable) components in formulations. Owing to the simple *in situ* generation of Co catalysts,[14] extremely low catalyst loading (ppm to ppk level) and facile post-synthesis deactivation of catalyst by air, CCTP has been widely adopted commercially to synthesize useful reactive oligomers. The incorporation of CCTP-derived reactive oligomers has been applied in adhesive and emulsion industries. Mitsubishi Chemical Corp. patented the use of CCTP-derived PMMA oligomers in resin compositions to improve adhesive performance.[15] It was found that a non-reactive copolymer which did not use CCTP weakened the materials, presumably due to the more random distribution of MMA moiety in the copolymer and loss of its hardening ability in the adhesive. Analogously, Rohm and Haas Co. also reported the use of methacrylic acid reactive oligomers from aqueous solution CCTP in poly(butyl acrylate) coatings, with the shear resistance significantly enhanced by the graft copolymers derived from the reactive oligomers compared to the MAA-BA copolymers.[16] 3M have commercialized a CCTP derived crosslinker known as an addition–fragmentation monomer (AFM) in dental resins to mitigate polymerization induced shrinkage and stress accumulation in dental resin.[17]

In academic research, D'Agosto has shown how PMMA reactive oligomers can be used to make PE-*b*-PMMA block

[a]*Halcyon3D Ltd, 27f Ignite House, Venture Centre, Coventry, CV4 7EZ, UK*
[b]*Department of Chemistry, University of Warwick, Coventry, CV4 7AL, UK.*
E-mail: D.M.Haddleton@warwick.ac.uk

† Electronic supplementary information (ESI) available. See DOI: https://doi.org/10.1039/d4py00482e

copolymers be effectively acting as a radical chain stopper in the radical polymerisation of ethene in both solution and emulsion.[18,19] When added to radical polymerisation of less reactive methacrylates they undergo very efficient RAFT to give multi block polymethacrylates again in both solution and emulsion polymerisation conditions.[20] The capabilities of these reactive oligomers has also been demonstrated by application in soap-free emulsion polymerization in the synthesis of functional nanoparticles.[21–23]

Conversely, 3D printing mediated by controlled radical polymerization has drawn only a small amount of attention. Boyer *et al.* investigated 3D printing mediated by RAFT derived macroinitiators and the effects of polymer architecture on the nanoscale segregation and mechanical properties.[24–26] Worrell has explored the addition of cobaloxime catalyst at ppm level in the 3D printing of dimethacrylates and achieved control in gel point and thermomechanical properties.[27]

Recently, we have reported the application of an addition–fragmentation monomer in 3D printing to improve shrinkage stress relaxation.[28] As an extension of this work, we aimed to investigate the versatility of CCTP-derived reactive oligomers in photolithographic 3D printing. Herein, we report the synthesis of reactive oligomers of ethylhexyl methacrylate (EHMA), poly(ethylene glycol)methacrylate (PEGMA) with different molecular weights and the effects of the addition of these to 3D printing resin formulations. It was found that when the reactive oligomer was compatible with the bulk monomer, the product was plasticized by the reactive oligomer leading to a weakened product. Meanwhile, an incompatible reactive oligomer resulted in a good reinforcement effect without significant mechanical deterioration. This current work offers a facile route to attain a broad spectrum of mechanical properties of 3D printing materials with low content (≤10% w/w) of additive.

Experimental details

Materials

Ethylhexyl methacrylate (98%), poly(ethylene glycol)methyl ether methacrylate (M_w: 300 g mol^{-1}), dimethylglyoxime (≥99%), isobornyl acrylate, poly(ethylene glycol)diacrylate (MW: 250 g mol^{-1}), poly(ethylene glycol)diacrylate (M_w: 700 g mol^{-1}) and alizarin were purchased from Sigma-Aldrich. Pyridine (Extra pure) and cobalt(II) acetate tetrahydrate (98%) were purchased from Fisher Scientific. Azobisisobutyronitrile (AIBN) (98%) was supplied by Wako chemicals. Phenylbis (2,4,6-trimethylbenzoyl)-phosphine oxide (BAPO) (96%) was supplied by Tokyo Chemical Industry UK Ltd. All chemicals were used as received.

Instrumentation

Size exclusion chromatography (SEC). SEC was performed on an Agilent 390-LC MDS instrument with $CHCl_3$ (or DMF containing 5 mM NH_4BF_4) as the mobile phase with 1 mL min^{-1} flow rate at 30 °C, equipped with a differential refractive index (DRI), viscometry (VS), dual angle light scatter (LS) and dual wavelength UV detectors, 2 PLgel mixed C (D) columns (300 × 7.5 mm) and a PLgel 5 μm guard column for separation and an autosampler for sample injection. Poly(methyl methacrylate) (Agilent EasyVials) were used for narrow standard calibration. All samples passed through 0.2 μm PTFE filter membrane prior to analysis.

Nuclear magnetic resonance spectroscopy (NMR). NMR was performed on Bruker Avance III 400 (resonance frequency of ^{1}H: 400 MHz). Deuterated chloroform and methanol were used as solvents for EHMA and PEGMA respectively. In a typical experiment of ^{1}H NMR, 2 dummy scans and 14 actual scans were performed with 4 s acquisition time and 1 s delay time per scan. In a typical ^{13}C NMR, 4 dummy scans and 124 actual scans were performed with 1.26 s acquisition time and 2 s delay time per scan.

DLP 3D printing. All objects were printed using "Anycubic D2 DLP" printer using the same parameters. In brief, the model was designed using Onshape online CAD software and exported as an .stl file (Fig. S.6†). Then the .stl file was sliced using Anycubic Photon Workshop software. The layer thickness was set as 50 μm. The bottom layer and normal layer printing time and off time were set as 25 s, 8 s and 5 s respectively. The pulling and retracting speed were set as 2 and 3 mm s^{-1} respectively.

ATR-FTIR spectroscopy. FTIR spectroscopy was performed on Bruker ALPHA II compact FT-IR spectrometer. In a single measurement, solid sample was loaded onto the diamond mirror, and 16 scans were performed for background and sample acquisition between 4000 and 400 cm^{-1} in transmittance mode. Spectra were first inverted to absorbance then normalized at 1725 cm^{-1} of the C=O stretching band.

Tensile testing. Tensile tests were performed on a Shimadzu EZ LX Universal Testing Instrument under ambient condition. In brief, a dog bone specimen was affixed to the instrument using cross-hatched sample holder. Then the specimen was subjected to vertical pulling at a speed of 30 mm min^{-1} until breakage. The ultimate stress (σ_T) and strain (γ_T) were recorded.

Owing to the inherent softness of the materials the Young's modulus from the linear fit of stress strain curve at low strain region (*ca.* 1%) was heavily susceptible to the region selected and errors due to insufficient measurement points. Herein, a method modified from Maláč's method was adopted to calculate the specific deformation energy by integrating the stress strain curve.[29,30] To mitigate the error by random selection, the point at local maximum stress, or the knee point when no local maximum was observed, was chosen as the reference point according to Kucherskii's method. The determination of knee point was as followed.[31] In brief, an empirical 15th order polynomial was fitted to the entire stress strain curve to minimize the noises, and the knee point was the minimum of the first derivative of the fitted curve (Fig. S.1†).

Dynamic mechanical thermal analyses (DMTA). DMTA was performed on a PerkinElmer DMA8000 equipped with a single cantilever geometry and hand-operated liquid nitrogen supply.

A rectangular specimen of 10 mm × 3 mm × 4 mm was load into single cantilever geometry. The specimen was subjected to an oscillation at a fixed frequency of 1 Hz and strain of 0.5% across the temperature range from −30 °C to 90 °C at a ramp rate of 3 °C min^{-1}.

Experimental procedures

Catalytic chain transfer polymerization (CCTP) of methylphenyls methacrylate. In a typical reaction, ethylhexyl methacrylate (150 g) and ethyl acetate (70 g) were charged in to a 3 neck round bottom flask equipped with a condenser. Cobalt(II) acetate tetrahydrate (6 mg), dimethylglyoxime (6 mg), and pyridine (0.15 mL) were added to the reaction mixture. Separately, AIBN stock solution was prepared by dissolving AIBN (2 g) in ethyl acetate (40 ml).

The reaction mixture and AIBN stock solution were deoxygenated by purging with N_2 for 1 h. The reaction mixture was then transferred to a 90 °C oil bath for 30 min to equilibrate the temperature and allow dissolution of the cobalt salts. AIBN solution (30 mL) was added into the reaction mixture using a N_2 filled syringe to initiate the reaction. The reaction was allowed to proceed for 3 h, then terminated by allowing to cool to ambient temperature and opened to air. The conversion and degree of polymerization were determined from ^{1}H NMR and the molecular weight distribution was acquired using SEC in chloroform.

The solvent and volatiles were removed by rotary evaporation at 50 °C and 150 mPa to remove most of the ethyl acetate. The product was obtained as a viscous liquid which was kept in a vacuum oven at 40 °C overnight to remove any residual volatiles. The product was stored at ambient conditions until use.

Free radical polymerization of EHMA mediated by ω-vinyl terminated reactive oligomers. In a typical reaction, PEHMA reactive oligomer synthesized *via* CCTP (20 g, 0.0202 mol) was dissolved in EHMA monomer (40 g, 0.202 mol) and AIBN (0.166 g, 1.01 mmol) was added. The reaction mixture was deoxygenated by purging with N_2 gas for 0.5 h, and the reaction was allowed to proceed at 85 °C oil bath for 4 h. The product was characterized using ^{1}H NMR and SEC to determine the conversion and molecular weight and used without further purification.

CCTP of poly(ethylene glycol)methyl ether methacrylate (PEGMA). In a typical reaction, PEGMA (150 g) was charged to a round bottom flask. Cobalt(II) acetate tetrahydrate (10 mg), dimethylglyoxime (10 mg), AIBN (1.5 g) and pyridine (0.15 mL) were added to the reaction mixture. The reaction mixture was deoxygenated by purging N_2 for 1 h prior to being transferred to an oil bath at 90 °C. The reaction was allowed to proceed for 3 h prior to termination by allowing to cool to ambient temperature open to air. The conversion and degree of polymerization were determined from ^{1}H NMR and the molecular weight distribution was acquired using SEC with DMF as eluent. The product was stored in ambient conditions until use.

Free radical polymerization of PEGMA mediated by ω-vinyl terminated reactive oligomers. In a typical reaction, PEGMA reactive oligomer synthesized *via* CCTP (30 g, 7.1 mmol) was dissolved in PEGMA monomer (30 g, 0.1 mol). AIBN (0.058 g, 0.36 mmol) was added to the reaction mixture. The reaction mixture was degassed by purging N_2 gas for 0.5 h, then the reaction was allowed to proceed at 85 °C oil bath for 4 h. The product was characterized using ^{1}H NMR and SEC to determine the conversion and molecular weight and used without further purification.

Resin formulations. All of the resin formulations were prepared by mixing all of the components directly into an sealed amber-coloured container. The resin was first subjected to vigorous agitation followed by mild sonication in a water bath for at least 15 min or until no visible solid residue remained. The resins were stored in the dark at ambient conditions until use. The resins compositions are summarized in Table 1. The nomenclature is specified as mX_n-Y, where m is the % w/w of reactive oligomers, X represents the type of additive reactive oligomers with the DP of n, of which O is the blank without the reactive oligomers, E is PEHMA reactive oligomers and P is PEGMA reactive oligomers. Y represents the crosslinker, where 1 means PEGDA (M_w: 250), 2 means 1 : 1 w/w mixture of PEGDA (M_w: 250 and 700), 3 means PEGDA (M_w: 700). For example, $10E_{15}$-1 means the base resin with 10% w/w $PEHMA_{15}$ reactive oligomers using PEGDA (M_w: 250) as crosslinker.

Table 1 Nomenclature and formulations of the resins

	Monomer	Crosslinker	Additive
O-1	66.7% IBoA	33.3% PEGDA 250	—
O-2	66.7% IBoA	16.7% PEGDA 250 16.7% PEGDA 700	—
O-3	66.7% IBoA	33.3% PEGDA 700	—
$10E_{15}$-1	56.7% IBoA	33.3% PEGDA 250	10% EHMA15
$10E_{15}$-2	56.7% IBoA	16.7% PEGDA 250 16.7% PEGDA 700	10% EHMA15
$10E_{15}$-3	56.7% IBoA	33.3% PEGDA 700	10% EHMA15
$5E_1$-2	61.7% IBoA	16.7% PEGDA 250 16.7% PEGDA 700	5% EHMA
$5E_5$-2	61.7% IBoA	16.7% PEGDA 250 16.7% PEGDA 700	5% $EHMA_5$
$5E_{15}$-2	61.7% IBoA	16.7% PEGDA 250 16.7% PEGDA 700	5% EHMA15
$5P_1$-2	61.7% IBoA	16.7% PEGDA 250 16.7% PEGDA 700	5% PEGMA
$5P_{14}$-2	61.7% IBoA	16.7% PEGDA 250 16.7% PEGDA 700	5% $PEGMA_{14}$
$5P_{28}$-2	61.7% IBoA	16.7% PEGDA 250 16.7% PEGDA 700	5% $PEGMA_{28}$
$10P_1$-2	56.7% IBoA	16.7% PEGDA 250 16.7% PEGDA 700	10% PEGMA
$10P_{14}$-2	56.7% IBoA	16.7% PEGDA 250 16.7% PEGDA 700	10% $PEGMA_{14}$
$10P_{28}$-2	56.7% IBoA	16.7% PEGDA 250 16.7% PEGDA 700	10% $PEGMA_{28}$

All % in w/w; all formulations contain an additional 1% w/w BAPO and 0.03% w/w alizarin as photoinitiator and photoabsorber respectively.

Results and discussion

Synthesis of reactive oligomers by CCTP and AFCT

ω-Vinyl terminated reactive oligomers of PEHMA and PEGMA were synthesized *via* CCTP and subsequent AFCT to attain different DP. The mechanism of CCTP and the subsequent AFCT mediated by the ω-vinyl terminated reactive oligomers were shown in Fig. S.2.† ^{1}H NMR spectra of the products were employed to determine the conversion and DP of the reactive oligomers calculated from eqn (1) and (2) for PEHMA and PEGMA respectively.

^{1}H NMR of the PEHMA reactive oligomer synthesized *via* CCTP is shown in Fig. S.5.† The conversion (X) and degree of polymerization (DP) was calculated by eqn (1). X and DP of the reactive oligomer by CCTP were 97.8% and 5 respectively, and 99.5% and 15 after chain extension of EHMA *via* AFCT. ^{1}H NMR (400 MHz, $CDCl_3$) δ = 0.60–1.00 (6H, CH-CH_2-CH_3 of EHMA and MM), 2.41–2.71 (α-CH_2-C═C-COOR), 3.75–4.25 (2H, O-CH_2 of EA, EHMA and MM), 5.40–5.59 (singlet, 1H, *trans* C═CH_2 of monomer and MM), 6.05–6.11 (1H, *cis* C═CH_2 of monomer), 6.13–6.26 (singlet, 1H, *cis* C═CH_2 of MM).

$$X = 1 - \frac{6\int_{6.05}^{6.11} 1\mathrm{H}}{\int_{0.60}^{1.00} 1\mathrm{H}};\ \mathrm{DP} = X\frac{\int_{0.60}^{1.00} 1\mathrm{H}}{6\int_{6.13}^{6.26} 1\mathrm{H}}\ \#\ \text{for EHMA} \quad (1)$$

^{1}H NMR of the PEGMA reactive oligomer synthesized *via* CCTP is shown in Fig. S.4.† The conversion (X) and degree of polymerization (DP) was calculated by eqn (2). X and DP of the reactive oligomer by CCTP were 90.0% and 14 respectively, and >99% conversion (non-detectable monomer by ^{1}H NMR) and 28 after chain extension of PEGMA *via* AFCT. ^{1}H NMR (400 MHz, $CDCl_3$) δ = 1.87–2.03 (3H, α-CH_3), 2.41–2.71 (α-CH_2-C═C-COOR), 3.27–3.44 (3H, CH_2O-CH_3), 3.45–3.59 (2H, CH_2O-CH_3), 3.59–3.71 (12H, –O-CH_2–), 3.71–3.82 (2H, O═C-OCH_2-CH_2O), 4.20–4.35 (2H, O═C-OCH_2), 5.40–5.59 (singlet, 1H, *trans* C═CH_2 of monomer and MM), 6.05–6.11 (1H, *cis* C═CH_2 of monomer), 6.13–6.26 (singlet, 1H, *cis* C═CH_2 of MM).

$$X = 1 - \frac{3\int_{6.05}^{6.11} 1\mathrm{H}}{\int_{3.45}^{3.27} 1\mathrm{H}};\ \mathrm{DP} = X\frac{\int_{3.45}^{3.27} 1\mathrm{H}}{6\int_{6.13}^{6.26} 1\mathrm{H}}\ \#\ \text{for PEGMA} \quad (2)$$

The molecular weight was determined by SEC in $CHCl_3$ using calibration using PMMA standards. The molecular weight distributions of the reactive oligomers as prepared by CCTP and after chain extension by AFCT are shown in Fig. S.4.† The M_n, M_w and dispersity ($Đ$) are summarized in Table 2.

Table 2 M_n, M_w and $Đ$ of PEHMA and PEGMA reactive oligomer determined using SEC in $CHCl_3$ with PMMA narrow standard, and DP and X determined using ^{1}H NMR (400 MHz)

	$M_{n,GPC}$	$M_{w,GPC}$	$Đ$	DP_{NMR}	X
$PEHMA_5$	1020	1950	1.91	5	97.8
$PEHMA_{15}$	2950	9400	3.18	15	99.5
$PEGMA_{14}$	4890	10 700	2.19	14	90.0
$PEGMA_{28}$	9600	35 600	3.70	28	>99

Tensile testing of the 3D printed parts

3D printings are performed with isobornyl acrylate and poly (ethylene glycol)diacrylate as the base resin. This is as acrylic monomers have a fast propagation rate which shortens printing time and gives better incorporation *via* the formation of comb polymer.[32] The specific choice of isobornyl acrylate is due to its high T_g and hydrophobicity. This facilitates storage without tackiness or softening by moisture. In addition, the resin can be handled safely in household ventilation due to the low volatility. PEGDA with different molecular weights were chosen to prevent hard and brittle materials beyond the instrumental limit for mechanical testing. All printed parts have been characterized by FT-IR spectroscopy to confirm the complete conversion by the disappearance of the band at 816 and 1636 cm^{-1} of the acrylic ═CH_2 and C═C from monomers (Fig. S.7†).

Tensile tests were performed to evaluate the effect of the crosslinker and additive type and its concentration. The specific tensile energy (U_T), stress (σ) and strain (ε) at the damaging point (or knee point; K in subscript) and the ultimate point (U in subscript) are summarized in Table S.2† (see tensile test in Experimental section for definition and details). The significance of the knee point is that the original configuration was mechanically overcome, and further external force would lead to either complete damage (for rigid material) or internal reconfiguration (strain hardening for elastomer), whereas the ultimate point referred to the breakage of the materials.

The base resin with a crosslinker with a different spacer length demonstrated a significant effect on the tensile properties (Fig. 1). σ_K and $U_{T,K}$ were 7.28, 26.78, 45.71 MPa and 443.51, 136.62 and 70.96 MPa for O-3, O-2 and O-1 (increasing PEGDA250: PEGDA 700), and at the ultimate breakage point, σ_U and $U_{T,U}$ were 12.64, 18.87, 44.39 MPa and 796.94, 415.97 and 502.30 MPa for O-3, O-2 and O-1 respectively. These results indicated that O-1 (with PEGDA 250 only) has the strongest initial structure against deformation before the knee point, then O-2 (1 : 1 w/w of PEGDA 250 and PEGDA700) and O-3 (PEGDA 700 only) the least. After the knee point, O-1 was damaged rapidly upon further elongation by 1.11% (6.52% of ε_K). Meanwhile, O-2 and O-3 can be further elongated by 13.03% (161% of ε_K) and 75.34 (661% of ε_K) respectively.

At the molecular level, low molecular weight PEGDA250 seems to form a compacted network with high crosslink density, reflected by the high stress and specific energy observed at the knee point. However, the short space length limits the extension of the material and therefore ultimate breakage occurs upon a slight elongation after the knee point. A less crosslinked, and consequently, a weaker network is formed by higher molecular weight PEGDA 700, at the same content by mass resulting in a smaller σ_K and $U_{T,K}$. However, the longer spacer of PEGDA 700 unfolds under stress to allow larger elongation prior to ultimate breakage. In order to signify the effect of additives, O-2 with the moderate properties was chosen as the base resin for later studies.

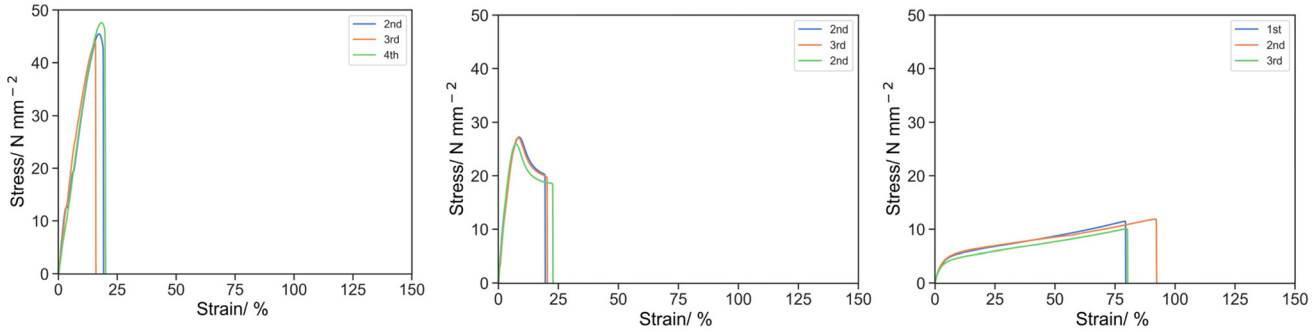

Fig. 1 Stress strain curve by tensile test for O-1 (left), O-2 (middle) and O-3 (right) under uniaxial tension at 50 mm s^{-1}.

ω-Vinyl terminated reactive oligomers were incorporated into the resins with a varied content, chemistry and molecular weight. 2-Ethylhexyl methacrylate and poly(ethylene glycol) methacrylate were selected here as low T_g materials with opposite hydrophilicity.

Initially, 10% w/w of IBoA was replaced by $PEHMA_{15}$ reactive oligomer (Fig. 2). For $10E_{15}$-1 (PEGDA 250 only) and $10E_{15}$-2 (1 : 1 PEGDA 250 and PEGDA 700), weakening was observed where σ_K and $U_{T,K}$ reduced to 20.58 MPa and 77.92 MPa at 6.53% for $10E_{15}$-1, and σ_K and $U_{T,K}$ reduced to 13.44 MPa and 73.77 MPa at 8.17% for $10E_{15}$-2. In both cases, complete breakage occurred after the knee point and no strain hardening was observed. For $10E_{15}$-3 (PEGDA 700 only), the material was in fact reinforced giving a similar knee stress but improved elongation, where σ_K and $U_{T,K}$ of O-3 were 6.38 and 102.26 MPa at 22.78% respectively. Similar strain-hardening was observed after the knee point where σ_U and $U_{T,U}$ were 11.07 and 644.54 MPa at 84.16%. The weakening effect observed with the $PEHMA_{15}$ reactive oligomer for $10E_{15}$-1 and $10E_{15}$-2 was attributed to low T_g of PEHMA and the polymerization kinetics of reactive oligomer with the oligomer incorporation. PEHMA has a T_g of −6 °C which softens the bulk material and reduces the specific energy. Kinetically, the rate of propagation of the reactive oligomer is slower than with the acrylic monomer resulting in a shorter kinetic primary chain length. Moreover, the reactive oligomers can also act as a chain transfer agent further reducing the kinetic chain length and thus crosslink density. The combination of these ultimately leads to weaker materials. No weakening effect was observed for $10E_{15}$-3 as the T_g of PEG spacer and the crosslink density of the material are already low in the base resin (O-3). Further introduction of low T_g component has negligible effect on the specific energy of the material.

Subsequently, the effect of the $PEHMA_{15}$ reactive oligomer concentration was investigated (Fig. 3). A clear trend in the reduction of σ_K and $U_{T,K}$ of 26.78, 19.31 and 13.44 MPa, and 136.62, 101.90, 73.77 MPa was observed with an increasing content of PEHMA15 from 0, 5 and 10% w/w, where the observed knee strain were almost identical at 8.10, 8.13 and 8.17%. At the ultimate point, the incorporation of 5% $PEHMA_{15}$ slightly reduced the stress from 18.87 MPa to 15.76 MPa but improved the strain from 21.13% to 25.77%, and therefore the toughness remained similar at 415.97 and 400.31 MPa respectively, whereas complete breakage was seen at 10% $PEHMA_{15}$ as previously mentioned.

It was postulated that $PEHMA_{15}$ was compatible with poly (isobornyl acrylate) based resin owing to the aliphatic character acting as a plasticizer. These phenomena were similar with the mechanical properties of miscible poly(vinyl chloride)/polycaprolactone blend reported by Chiu and Min.[32] The suppression and subsequently disappearance of the yielding behaviour was attributed to the reduction of T_g by $PEHMA_{15}$. This enhanced the mobility of polymer segments allowing for longer extension with the compromise on lower stress. At

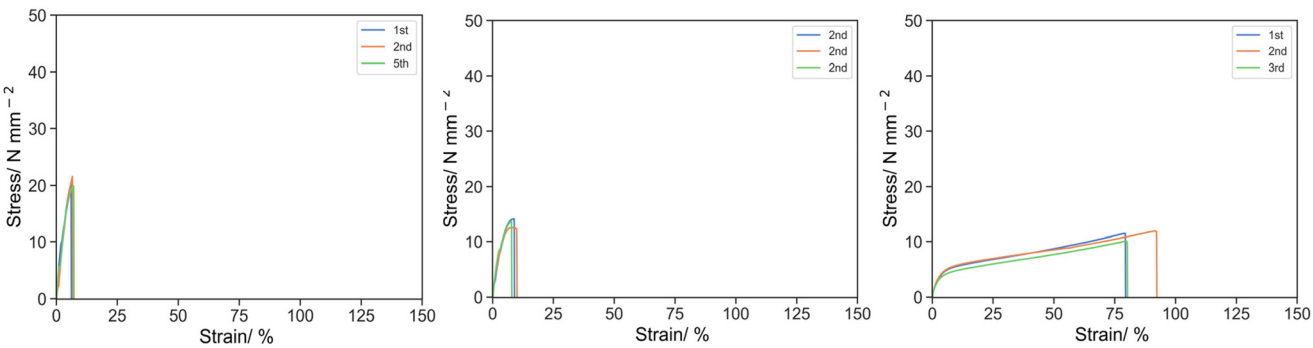

Fig. 2 Stress strain curve for $10E_{15}$-1 (left), $10E_{15}$-2 (middle) and $10E_{15}$-3 (right) under uniaxial tension at 50 mm s^{-1}.

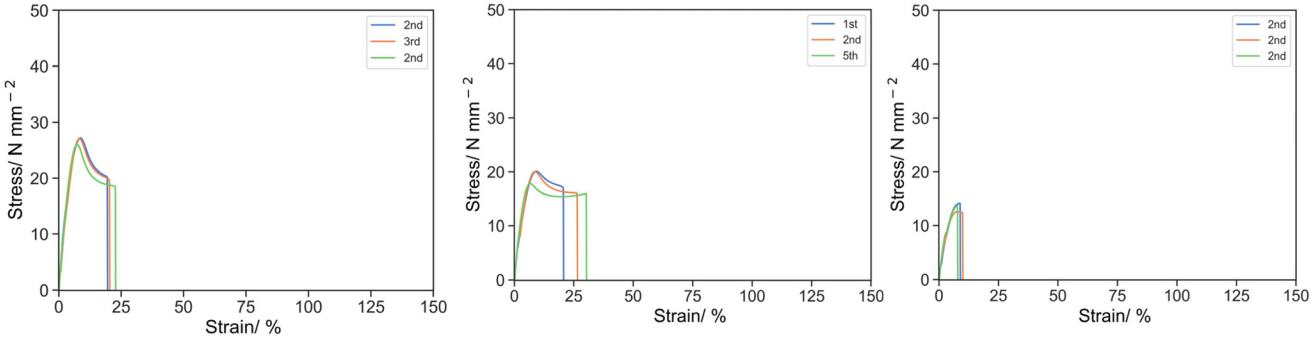

Fig. 3 Stress strain curve for O-2 (left), $5E_{15}$-2 (middle) and $10E_{15}$-2 (right) under uniaxial tension at 50 mm s^{-1}.

higher reactive oligomer content (10% w/w), the crosslink density is significantly reduced due to the chain transfer activity and slower polymerization rate, and only weakening was observed. Therefore, 5% w/w additive was chosen for later studies.

The effect of the molecular weight of the reactive oligomers was demonstrated by $5E_1$-2, $5E_5$-2 and $5E_{15}$-2, using EHMA monomer, PEHMA5 and PEHMA15 reactive oligomer respectively (Fig. 4). It was observed that the molecular weight of the reactive oligomer had little but significant effect on the knee point with the stress of 23.88, 21.93, 19.31 MPa; strain of 8.44, 8.12, 8.13% and specific energy of 126.81, 112.04 and 101.90 MPa for EHMA, $PEHMA_5$ and $PEHMA_{15}$ respectively.

However, at the ultimate point, $5E_5$-2 appears to be the weakest material with σ_U, ε_U and $U_{T,U}$ of 17.85 MPa, 17.92% and 302.25 MPa respectively, followed by $5E_{15}$-2 with σ_U, ε_U and $U_{T,U}$ of 15.76 MPa, 25.77% and 400.31 MPa. $5E_1$-2 was the strongest among, with σ_U, ε_U and $U_{T,U}$ of 19.01 MPa, 34.21% and 635.06 MPa respectively.

The variation in the mechanical properties can be rationalized by the polymerization kinetics. Moad *et al.* and Yamada *et al.* have studied the kinetics of propagation and chain transfer of ω-vinyl terminated reactive oligomers and concluded that whereas the k_p drops considerably and the chain transfer activity increases from monomer to dimer, then approaches constant for further higher molecular weight.[33–36] Therefore, $PEHMA_5$ and $PEHMA_{15}$ reactive oligomer induced a lower degree of crosslinking than EHMA due to slower propagation and chain transfer activity, and weaken the material. Then regarding $PEHMA_5$ and $PEHMA_{15}$, the k_p and k_{ct} are similar but since $PEHMA_5$ has a lower molecular weight, the molar concentration of reactive oligomer in $5E_5$-2 will be higher than $5E_{15}$-2, at the same mass fraction of reactive oligomer, and thus $5E_5$-2 had the slowest polymerization and degree of crosslinking and formed the weakest material.

The effect of the chemistry of the reactive oligomer was also investigated. $(PEGMA)_{14}$ which has a similar M_w to $PEHMA_{15}$ was synthesized *via* CCTP, but more polar than the aliphatic EHMA and IBoA and incorporated into the resin (Fig. 5) and has a methacrylic end group so acts as a true macromonomer (MM).

The mechanical properties were distinctive to its equivalence of $PEHMA_{15}$. Despite the similar suppression of the stress, the elongation of the materials was significantly improved by the inclusion of $PEGMA_{14}$. σ_K was 26.78, 17.61 and 13.16 for O-2, $5P_{14}$-2 and $10P_{14}$-2 respectively, whereas ε_K was 8.10, 8.06 and 9.93, and $U_{T,K}$ was 136.62, 95.10 and 95.61 respectively. For the ultimate point, σ_U was 18.87, 16.47 and 14.06 for O-2, $5P_{14}$-2 and $10P_{14}$-2 respectively, whereas ε_K was 21.13, 39.61 and 38.79, and $U_{T,K}$ was 415.97, 609.65 and 495.59 respectively.

One of the explanations could be the phase separation of the more polar PEG moiety from aliphatic isobornyl acrylate. Reinforcement by polymerization-induced phase separation

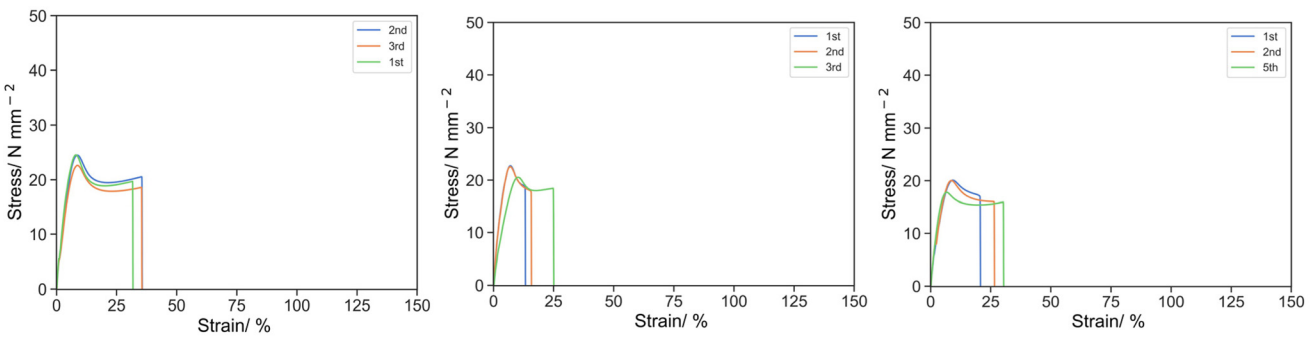

Fig. 4 Stress strain curve for $5E_1$-2 (left), $5E_5$-2 (middle) and $5E_{15}$-2 (right) under uniaxial tension at 50 mm s^{-1}.

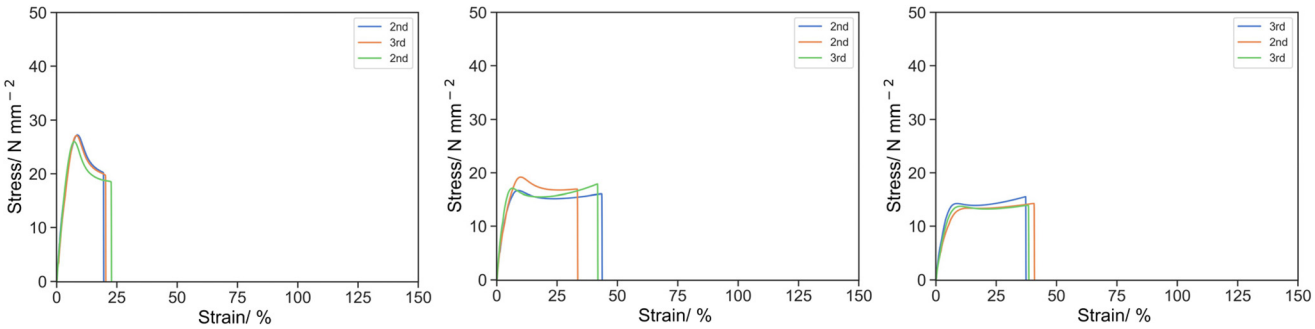

Fig. 5 Stress strain curve for O-2 (left), $5P_{14}$-2 (middle) and $10P_{14}$-2 (right) under uniaxial tension at 50 mm s^{-1}.

has long been studied in the case of high-impact polystyrene and PMMA/epoxy.[37–40] Upon phase separation, the continuous phase remains predominantly hard component of isobornyl acrylate to contribute to the mechanical strength of the material, whereas the segregated soft component of $(PEGMA300)_{14}$ enhances the elongation prior to the breakage. As the content of $(PEGMA300)_{14}$ further increased, the soft phase tended to be continuous which would no longer enhance the ductility, instead a larger fraction of it also incorporated into the hard phase *via* copolymerization with isobornyl acrylate, led to the plasticization and softening of the material which lowered the specific energy and strength of the material.

The effects of PEGMA reactive oligomers at different molecular weights were also demonstrated (Fig. 6). At the knee point, the stress increased 7.65, 13.76 and 17.1 for 10-P1-2, 10-P14-2 and 10-P28-2, and the strain decreased 21.17, 9.93 and 9.35, which gave the specific energy of 102.26, 95.61 and 109.27 respectively. Similar trend was observed at the ultimate point, the stress was 11.23, 14.06 and 15.08, whereas the strain was 71.69, 38.79 and 30.37, and the specific energy was 615.18, 495.59 and 442.10 for $10P_1$-2, $10P_{14}$-2 and $10P_{28}$-2 respectively.

The rise in the knee stress and shift toward the smaller strain suggested that the structure became harder and more brittle. It was postulated that the change in mechanical properties were attributed to the polymerization-induced phase separation. In addition to the intrinsic localization in reactive oligomer, in theory, the higher the molecular weight, the more favoured the phase separation due to the higher entropy of phase separation in an incompatible polymer blend. Correlating to the mechanical properties, [monomer] demonstrated elastomeric properties with superior elongation and strain hardening before breakage. With an increase in the molecular weight of the reactive oligomer from DP = 1 to 14 then 28, the material transformed from an elastomer to a tougher and more brittle material. It was elucidated that the degree of phase separation was minuscule and a larger fraction of PEGMA was incorporated into the continuous phase and lower the T_g when PEGMA monomer was employed, resulting a ductile elastomer with the sign of superior elongation and strain hardening prior to breakage. As the molecular weight of the reactive oligomer increased, the PEGMA moiety was more favoured to phase separate from the continuous phase and resulting in a larger fraction of hard component of poly(isobornyl acrylate) remaining in the continuous phase, at the same total content of additive, and eventually led to the reduction in elongation and improvement in the mechanical strength and specific energy. Similar effects of phase separation, controlled by annealing time and temperature, on mechanical properties in polystyrene/poly(vinyl methyl ether) blend were also observed by Kim and Karasz.[41]

Dynamic mechanical and thermal analyses (DMTA)

DMTA was carried out to further understand the relaxation and the microstructures of the printed parts. The loss factor ($\tan d$), the ratio of loss modulus to storage modulus (G''/G'), is a parameter related to the segmental motions, and any relaxation event raises a peak in $\tan s$. The temperature at

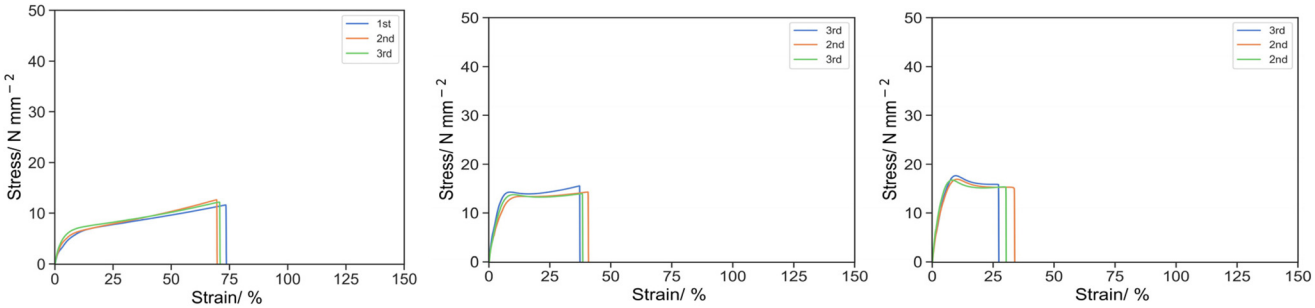

Fig. 6 Stress strain curve for $10P_1$-2 (left), $10P_{14}$-2 (middle) and $10P_{28}$-2 (right) under uniaxial tension at 50 mm s^{-1}.

maximum tan δ ($T_{max,\ tan\delta}$) and its characteristic width at 25% height ($\delta T_{25\%}$) represent the occurrence of a relaxation event and its span over a temperature range (Table S.3†). The interpretation of DMTA spectra will be based on the T_g and polymeric architecture. In brief, we herein used high T_g polymer (PIBOA, T_g: 86 °C) and low T_g reactive oligomeric additive (PEHMA or PEGMA T_g: −6 °C and −73 °C respectively), and the peak and width of tan δ indicate the T_g where segmental relaxation occurs and the degree of miscibility of the bulk polymer and the reactive oligomers. Typically, a narrow peak of tan δ suggests a homogeneously distributed bulk polymer and the reactive oligomers. As two components segregating, peak of tan δ starts broadening and eventually separate to two peaks at the T_g of the oligomers enriched and deficient domains respectively. This will give better insight to understand the origin of the tensile properties in molecular level, and the details of each formulation will be discussed as below.

The effect of the crosslinker was first demonstrated (Fig. 7). With an increasing amount of PEGDA700: PEGDA250, tan δ moving to lower temperature from 74.1 to 61.8 and 44.0 °C and the width of 25% peak height broadened from 17.2 to 18.3 and 23.9 °C for O-3, O-2 and O-1 respectively. As the fraction of PEGDA 700 increased, at the same total mass content of the crosslinker, the crosslink density reduced and thus enhanced the segmental mobility. Additionally, the extended PEG spacer length plasticizes the material to shift and broaden the peak tan_δ towards lower temperature.

The incorporation of 10% w/w $PEHMA_{15}$ reactive oligomer demonstrated different effects on the materials with different crosslink density (Fig. 8). Minuscule effects were observed on $10E_{15}$-1 apart from a small reduction $T_{max,\ tan\delta}$ (74.1 to 70.1 °C). In contrast, the $10E_{15}$-2 and $10E_{15}$-3 showed significant reduction in the $T_{max,\ tan\delta}$ from 61.8 and 44.0 °C to 55.1 and 35.7 respectively. Moreover, significant broadening was observed in $10E_{15}$-2 from 18.3 °C to 33.4 °C for $dT_{25\%}$.

It was postulated that at high crosslink density, the segmental mobility was constrained by covalent bonding predominantly instead of the glass transition of polymer compositions; therefore, additional PEHMA reactive oligomer does not have a significant effect on the segmental mobility. As the crosslink density is reduced from $10E_{15}$-1 to $10E_{15}$-3, the glass transition of the bulk polymer gradually predominated the mechanical properties, and the plasticization effect by the reactive oligomer became more significant.

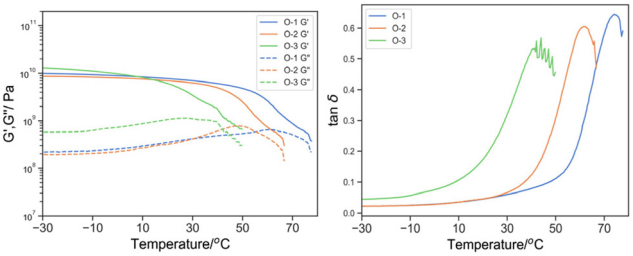

Fig. 8 Left: G' (solid line) and G'' (dotted line) by DMTA of O-1 (blue), O-2 (green), O-3 (orange); and right: its derived tan δ.

Considering the concentration of $PEHMA_{15}$ (Fig. 9), a clear shift in the $T_{max,\ tan\delta}$ to a lower temperature (61.8 °C for O-2, 57.8 °C for $5E_{15}$-2 and 55.1 °C for $10E_{15}$-2), peak broadening ($\delta T_{25\%}$: 17.2 °C for O-2, 22.7 °C for $5E_{15}$-2 and 33.4 °C for $10E_{15}$-2) was observed with increasing $PEHMA_{15}$. This further signified the role of EHMA15 as a plasticizer in the 3D printed parts. Similar shift and broadening has been observed in DMTA of tetraglyme solvated polyurethane.[42]

The effect of the molecular weight of reactive oligomer was investigated by incorporating 5% w/w of EHMA monomer, $PEHMA_5$ and $PEHMA_{15}$ reactive oligomer (Fig. 10). The molecular weight dependence of the relaxation spectra is subtle but we think significant. It was observed that $T_{max,\ tan\delta}$ moved to high temperature from 53.8 to 54.6 and 57.8 °C was accompanied by broadening and the appearance of a secondary shoulder as the molecular weight of the reactive oligomers increased from $5E_1$-2, $5E_5$-2 to $5E_{15}$-2. While it was minimal (compared to PEGMA as discussed later), the peak broadening and eventually separation suggested the uneven distribution of plasticizing comonomer when reactive oligomers were employed, and the degree of inhomogeneity increased with the molecular weight. It was postulated that despite the chemical similarity of aliphatic isobornyl acrylate and EHMA, the reactive oligomer created localized EHMA-rich domains depleted the EHMA content in the bulk phase, resulting a higher $T_{max,tan\delta}$ and peak broadening.

The incorporation of chemically incompatible and the more polar PEGMA reactive oligomers was then studied

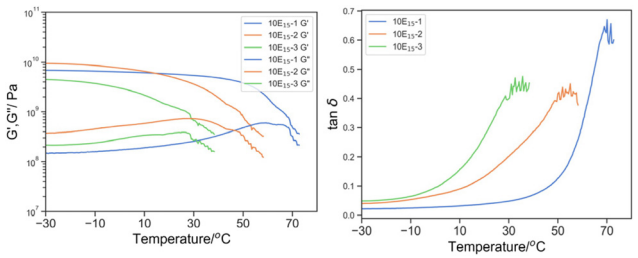

Fig. 7 Left: G' (solid line) and G'' (dotted line) by DMTA of $10E_{15}$-1 (blue), $10E_{15}$-2 (green), $10E_{15}$-3 (orange); and right: its derived tan δ.

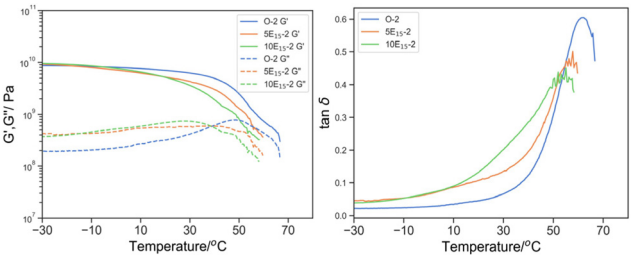

Fig. 9 Left: G' (solid line) and G'' (dotted line) by DMTA of O-2 (blue), $5E_{15}$-2 (green), $10E_{15}$-2 (orange); and right: its derived tan δ.

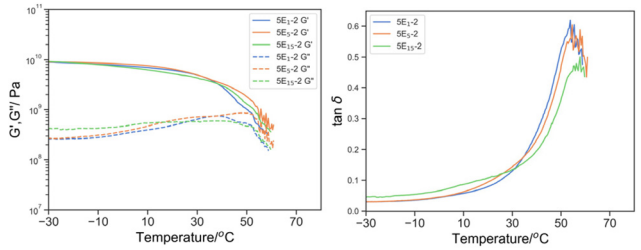

Fig. 10 Left: G' (solid line) and G'' (dotted line) by DMTA of $5E_1$-2 (blue), $5E_5$-2 (green), $5E_{15}$-2 (orange); and right: its derived tan δ.

(Fig. 11). The effects of PEGMA reactive oligomers were less noticeable than PEHMA reactive oligomer despite similar shifts in $T_{max,\ tan\delta}$ towards lower temperature with increasing content of $PEGMA_{14}$ reactive oligomer. Even at 10% w/w of reactive oligomer, only a slight secondary shoulder was observed between −10 and 30 °C, in contrast to the conspicuous broadening observed with 10% $PEHMA_{15}$.

Whilst regrettably the glass transition temperature of PEGMA (−60 °C) was beyond our instrument limit, one can expect that if PEGMA reactive oligomer incorporated into the bulk material as plasticizer in the same manner as EHMA, the downshift and broadening in tan_δ would be more pronounced. Conversely, $T_{max,\ tan\delta}$ of $10P_{14}$-2 (54.1 °C) was in fact similar with $10E_{15}$-2 (55.1 °C) and $\delta T_{25\%}$ was much narrower (21.7 °C *vs.* 33.4 °C), implying a lower content of PEGMA as plasticizer in the bulk material and the majority was phase separated to create PEGMA-rich domain whose T_g beyond the temperature range.

The concentration dependence of the $PEGMA_{14}$ reactive oligomer also suggested that only a small fraction was incorporated into the bulk material (Fig. 12). The subtle reduction in T_{max}, tan_δ from 61.8 to 60.1 and 54.1 °C at 5% w/w and 10% w/w $PEGMA_{14}$ respectively and the lack of broadening in tan δ induced by plasticization suggested that the content of $PEGMA_{14}$ had insignificant effect on the bulk material. The enhanced phase separation observed with higher molecular weight reactive oligomer was more prominent with PEGMA (Fig. 13). This was demonstrated by the shift in the peak tan d approaching the blank as its molecular weight increased, suggesting the content of PEGMA reactive oligomer reduced in

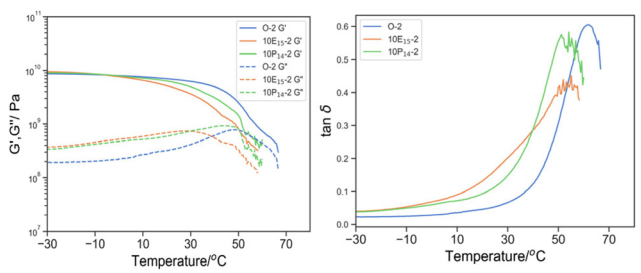

Fig. 11 Left: G' (solid line) and G'' (dotted line) by DMTA of O-2 (blue), $10E_{15}$-2 (green), $10P_{14}$-2 (orange); and right: its derived tan δ.

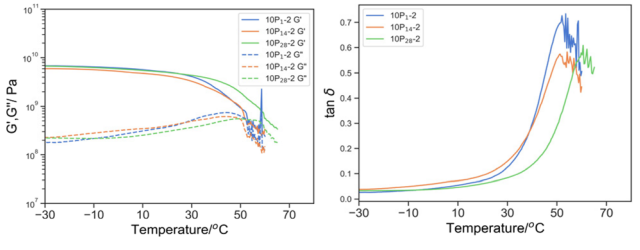

Fig. 12 Left: G' (solid line) and G'' (dotted line) by DMTA of $10P_1$-2 (blue), $10P_{14}$-2 (green), $10P_{28}$-2 (orange); and right: its derived tan δ.

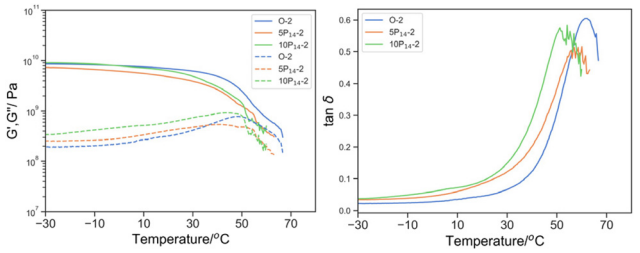

Fig. 13 G' (solid line) and G'' (dotted line) by DMTA of O-2 (blue), $5P_{14}$-2 (green), $10P_{14}$-2 (orange); and right: its derived tan δ.

the bulk material. The $T_{max,tan\delta}$ of 10-P_1-2, 10-P_{14}-2 and 10-P_{28}-2 was 53.6, 54.1 and 60.6 °C respectively, where the base resin (O-2) was 61.8 °C. The absence of peak broadening of tan δ, and in fact narrowing in 10-P_{28}-2, at any molecular weight of PEGMA reactive oligomer further illustrated that the bulk material is independent to the PEGMA reactive oligomer and indicated phase separation.

Conclusion

In this study, PEHMA and PEGMA reactive oligomers have been synthesized *via* CCTP mediated by the *in situ* formation of cobaloxime and used to mediate subsequent addition–fragmentation chain transfer (AFCT). The reactive oligomers have been incorporated into 3D printing resins as polymerizable additives. The effects of the chemistry, molecular weight and the concentration of reactive oligomer on the mechanical properties has been studied *via* tensile tests and the dynamic mechanical and thermal analyses and compared to the incorporation of the original monomer. It was found that PEHMA reactive oligomers were compatible with the isobornyl acrylate based resin and acted as a plasticizer in the bulk material. This caused the weakening of the material in tensile test with the reduction in stress, specific energy and elongation. Conversely, PEGMA based additive transformed the printed parts from brittle to ductile hard materials and further to true elastomers. The origin of such transition was postulated to be the phase separation of polar PEG moiety from the aliphatic isobornyl acrylate resin. The current approach opens a facile route to access a wide range of mechanical properties of DLP

3D printed parts across using a small quantity (up to 10% w/w) of additive.

Author contributions

Wai Hin Lee: writing – original draft, methodology, investigation, software, methodology, investigation, formal analysis, data curation, conceptualization. Zhongyuan Wan: methodology, investigation, data curation. Ataulla Shegiwal: writing, review & editing, visualization, supervision, resources, project administration, methodology, investigation. David Haddleton: writing, review & editing, visualization, supervision, resources, project administration, methodology, investigation, funding acquisition, conceptualization.

Data availability

The data supporting this article have been included as part of the ESI† and are available from the authors on request.

Conflicts of interest

DMH and AS are shareholders in Halcyon3D Ltd.

Acknowledgements

Funding was received from Halcyon3D Ltd and equipment used was funded in part by EPSRC *via* the Polymer Characterisation Research Technology Platform (RTP) of the University of Warwick EP/V036211/1 and EP/V007688/1.

References

1 R. Chaudhary, P. Fabbri, E. Leoni, F. Mazzanti, R. Akbari and C. Antonini, *Prog. Addit. Manuf.*, 2023, **8**, 331–351.
2 M. Manoj Prabhakar, A. K. Saravanan, A. Haiter Lenin, I. Jerin leno, K. Mayandi and P. Sethu Ramalingam, *Mater. Today: Proc.*, 2021, **45**, 6108–6114.
3 M. Pagac, J. Hajnys, Q.-P. Ma, L. Jancar, J. Jansa, P. Stefek and J. Mesicek, *Polymers*, 2021, **13**, 598.
4 W. Li, Y. Wu, W. Liang, B. Li and S. Liu, *ACS Appl. Mater. Interfaces*, 2014, **6**, 5726–5734.
5 W. Wang, R. Peng, Y. Gao, J. Nie and F. Sun, *Macromol. Chem. Phys.*, 2023, **224**, 2200458.
6 J. Cheng, Y. Cao, S. Jiang, Y. Gao, J. Nie and F. Sun, *Ind. Eng. Chem. Res.*, 2015, **54**, 5635–5642.
7 B. K. Kim, S. H. Kim and J. C. Song, *Polymer*, 1998, **39**, 5949–5959.
8 Y. Wang, C. Li, X. Tuo, Y. Gong and J. Guo, *J. Appl. Polym. Sci.*, 2021, **138**, 50102.
9 W. Geurtsen, W. Spahl and G. Leyhausen, *J. Biomed. Mater. Res.*, 1999, **44**, 73–77.
10 H. Lygre, K. N. Klepp, E. Solheim and N. R. Gjerdet, *Acta Odontol. Scand.*, 1994, **52**, 150–156.
11 N. S. Enikolopyan, B. R. Smirnov, G. V. Ponomarev and I. M. Belgovskii, *J. Polym. Sci., Polym. Chem. Ed.*, 1981, **19**, 879–889.
12 A. Gridnev, *J. Polym. Sci., Part A: Polym. Chem.*, 2000, **38**, 1753–1766.
13 A. A. Gridnev and S. D. Ittel, *Chem. Rev.*, 2001, **101**, 3611–3660.
14 Du Pont, *United States*, **4694054A**, 1987.
15 Mitsubishi Plastics Inc, *United States*, **9809731B2**, 2017.
16 Rohm & Haas, *United States*, **6864309B2**, 2005.
17 Du Pont, *United States*, **5028677A**, 1991.
18 F. Baffie, G. Patias, A. Shegiwal, F. Brunel, V. Monteil, L. Verrieux, L. Perrin, D. M. Haddleton and F. D'Agosto, *Angew. Chem.*, 2021, **133**, 25560–25568.
19 L. Sinniger, O. Boyron, P. Y. Dugas, G. Patias, D. Lester, D. M. Haddleton, V. Monteil, M. Lansalot and F. D'Agosto, *Polym. Chem.*, 2023, **14**, 4569–4579.
20 N. G. Engelis, A. Anastasaki, G. Nurumbetov, N. P. Truong, V. Nikolaou, A. Shegiwal, M. R. Whittaker, T. P. Davis, D. M. Haddleton, A. Anastasaki, G. Nurumbetov, N. P. Truong, V. Nikolaou, A. Shegiwal, M. R. Whittaker, T. P. Davis and D. M. Haddleton, *Nat. Chem.*, 2017, **9**, 171–178.
21 W. H. Lee, J. R. Booth and S. A. F. Bon, *Biomacromolecules*, 2020, **21**, 4599–4614.
22 A. Lotierzo, R. M. Schofield and S. A. F. Bon, *ACS Macro Lett.*, 2017, **6**, 1438–1443.
23 A. Lotierzo, B. W. Longbottom, W. H. Lee and S. A. F. Bon, *ACS Nano*, 2019, **13**, 399–407.
24 V. A. Bobrin, Y. Yao, X. Shi, Y. Xiu, J. Zhang, N. Corrigan and C. Boyer, *Nat. Commun.*, 2022, **13**, 3577.
25 V. A. Bobrin, K. Lee, J. Zhang, N. Corrigan and C. Boyer, *Adv. Mater.*, 2022, **34**, 2107643.
26 X. Shi, Y. Yao, J. Zhang, N. Corrigan and C. Boyer, *Small*, 2023, 2305268.
27 N. R. Bagnall, M. H. Jones, G. C. Jernigan, C. Routt, L. C. Dar and B. T. Worrell, *J. Am. Chem. Soc.*, 2023, **145**, 14202–14207.
28 Z. Wan, W. Lee, A. Shegiwal and D. Haddleton, *Eur. Polym. J.*, 2023, **196**, 112324.
29 J. Maláč, *Polym. Test.*, 2005, **24**, 790–792.
30 J. Maláč, *Polym. Test.*, 2006, **25**, 650–655.
31 A. M. Kucherskii, *Polym. Test.*, 2003, **22**, 503–507.
32 F.-C. Chiu and K. Min, *Polym. Int.*, 2000, **49**, 223–234.
33 C. L. Moad, G. Moad, E. Rizzardo and S. H. Thang, *Macromolecules*, 1996, **29**, 7717–7726.
34 J. Krstina, G. Moad, E. Rizzardo, C. L. Winzor, C. T. Berge and M. Fryd, *Macromolecules*, 1995, **28**, 5381–5385.
35 T. Harada, P. B. Zetterlund and B. Yamada, *J. Polym. Sci., Part A: Polym. Chem.*, 2004, **42**, 597–607.
36 B. Yamada, S. Tagashira and S. Aoki, *J. Polym. Sci., Part A: Polym. Chem.*, 1994, **32**, 2745–2754.
37 B. J. P. Jansen, S. Rastogi, H. E. H. Meijer and P. J. Lemstra, *Macromolecules*, 1999, **32**, 6283–6289.
38 B. J. P. Jansen, S. Rastogi, H. E. H. Meijer and P. J. Lemstra, *Macromolecules*, 2001, **34**, 4007–4018.

39 B. J. P. Jansen, S. Rastogi, H. E. H. Meijer and P. J. Lemstra, *Macromolecules*, 2001, **34**, 3998–4006.
40 B. J. P. Jansen, S. Rastogi, H. E. H. Meijer and P. J. Lemstra, *Macromolecules*, 2001, **34**, 3998–4006.
41 J. H. Kim, F. E. Karasz and M. F. Malone, *Polym. Eng. Sci.*, 1991, **31**, 981–987.
42 S. T. C. Ng, C. Jolliffe, A. Goodwin, M. Forsyth and D. R. MacFarlane, *Electrochim. Acta*, 1998, **43**, 1499–1503.